AIAA JOURNAL
Vol. 38, No. 11, November 2000

Postbuckling Analysis of Composite Laminated Panels

D. J. Dawe*
University of Birmingham, Edgbaston, Birmingham, England B15 2TT, United Kingdom
and
S. Wang†
Loughborough University, Loughborough, England LE11 3TU, United Kingdom

A description is given of the development of a spline finite strip method for predicting the response of composite laminated, prismatic panels to a progressive uniform end shortening. The response is assumed to be geometrically nonlinear, with the nonlinearity introduced in enhanced strain–displacement equations in a total Langrangian approach. The set of nonlinear equilibrium equations, obtained by appropriate energy minimization, is solved using the Newton–Raphson method. The development of the properties of a flat finite strip is made in the contexts of both first-order shear deformation plate theory and classical plate theory, and a number of strip models is available corresponding to different displacement fields. Presented applications concern a box section and several longitudinally stiffened panels that include curved panels modeled as faceted shells. Comparison of the finite strip predictions is made, where possible, with results from other sources, and such comparison is shown to be close.

Nomenclature

A	=	length of structure
A_{rs}, B_{rs}, D_{rs}	=	laminate stiffness coefficients
b	=	width of a finite strip
$\boldsymbol{d}$, $\bar{\boldsymbol{d}}$	=	column matrices of strip and structure freedoms, respectively
E_L, E_T	=	ply elastic moduli along and across fibers, respectively
G_{LT}, G_{TT}	=	shear moduli in plane of fibers and through the thickness, respectively
h	=	plate thickness
j	=	number of a reference line
$\boldsymbol{K}$, $\boldsymbol{K}_1$, $\boldsymbol{K}_2$, $\boldsymbol{K}^*$	=	strip stiffness matrix contributions
$\bar{\boldsymbol{K}}$, $\bar{\boldsymbol{K}}_1$, $\bar{\boldsymbol{K}}_2$, $\bar{\boldsymbol{K}}^*$	=	structure stiffess matrix contributions
$\bar{\boldsymbol{K}}_T$	=	tangent stiffness matrix for structure
k	=	degree of B-spline function basis
$k_i k_j$	=	shear correction factors
M	=	number of reference lines of a finite strip
N_{av}	=	average longitudinal force
N_j, N_{jH}	=	Lagrangian and Hermitian shape functions, respectively
NS	=	number of finite strips
n	=	degree of crosswise polynominal representation
$\boldsymbol{Q}$	=	matrix of stiffness coefficients for a ply
Q_{rs}	=	ply stiffness coefficients
q	=	number of spline sections in the structure length
U_p	=	strain energy of a strip
u, v, w	=	middle-surface displacements in the x, y, and z directions, respectively
u', v', w'	=	displacements in the x', y', and z' directions, respectively
$\boldsymbol{V}$, $\bar{\boldsymbol{V}}$	=	column matrices of contants for strip and structure, respectively
x, y, z	=	local coordinate axes
x', y', z'	=	global coordinate axes
α	=	angle between global and local axes
ε	=	applied uniform end-shortening strain
ε_x, ε_y, γ_{yz}, γ_{zx}, γ_{xy}	=	components of strain at a general point
ν_{LT}	=	major Poisson's ratio of a ply
$\boldsymbol{\sigma}$, $\boldsymbol{\varepsilon}$	=	column matrices of stress and strain, respectively
σ_x, σ_y, τ_{yz}, τ_{zx}, τ_{xy}	=	components of stress at a general point
$\bar{\Phi}_k$	=	modified B-spline function basis of degree k
ψ_x, ψ_y, ψ_z	=	rotations in the local system
$\psi_{x'}$, $\psi_{y'}$, $\psi_{z'}$	=	rotations in the global system

Received 24 November 1999; revision received 14 March 2000; accepted for publication 14 March 2000.

*Professor of Structural Mechanics, School of Civil Engineering.
†Lecturer in Structural Mechanics, Department of Aeronautical and Automotive Engineering.

Introduction

PRISMATIC plate and shell structures of rectangular planforms, such as stiffened panels, box sections, etc., are used frequently as load-bearing structural components in a number of engineering areas. In some such areas, notably aerospace and marine engineering, the structures may be made of fiber-reinforced composite laminated materials. The efficient design of these structures may need to be based on the assumption of nonlinear response to loading, and often of particular concern is the accurate prediction of buckling and postbuckling response to prescribed in-plane strain, such as that due to progressive end shortening. The finite strip method (FSM) offers the prospect of such prediction, and its development for forecasting the postbuckling response of plate structures is the subject of the present study.

The FSM is an analysis procedure that is particularly well suited to the solution of problems involving prismatic structures of relatively thin-walled construction. The method is, of course, a special form of the general finite element method (FEM), but it can have considerable advantages of efficiency and economy relative to the FEM. The FSM is very well established in the realm of linear analysis. A recent review by Dawe[1] describes in detail the use of the method in predicting the buckling stresses of composite-laminated plates and, to a lesser extent, of plate structures. There, two popular versions of the FSM are discussed, which differ in the nature of the variation of the assumed displacement field along the strip. These are the semi-analytical FSM (which uses continuous analytical functions longitudinally) and the spline FSM (which uses local spline functions longitudinally). For both of these versions, the strip properties can be developed in the context of the classical plate theory (CPT), or of a shear deformation plate theory (SDPT), which is inevitably more complicated, but is more realistic when dealing with composite laminates because through-thickness shear deformation is accounted for. More than one shear deformation theory exists, but the most commonly used is the first-order (Reissner–Mindlin) theory, which is the simplest one in the category.

The FSM has also found usage in nonlinear analysis, particularly with regard to postbuckling behavior. Early works concerned with the use of the semi-analytical FSM are those of Graves-Smith and

Sridharan,[2] Sridharan and Graves-Smith,[3] and Hancock.[4] These authors considered the post-local-buckling behavior of homogeneous plate structures with diaphragm ends when subjected to progressive end shortening, in the context of CPT. Dawe et al. (see Refs. 5–10) have used the semi-analytical FSM in considering the post-buckling behavior of composite laminated structures in the contexts of both CPT and the more refined first-order SDPT. These analyses relate to single plates,[5–8] to the post-local-buckling of plate structures,[9] and to the post-overall-buckling of diaphragm-supported plate structures.[10] The developed semi-analytical FSM capabilities are accurate and efficient, but there are restrictions on their use, which are caused by the specific nature of the assumed analytical, longitudinal variations of displacements, as regards the range of end conditions and of types of lamination that can be accommodated. The alternative spline FSM is much more versatile in these matters and is the approach adopted in this study.

The spline FSM, using B-spline functions, was introduced by Cheung and Fan[11] and Fan and Cheung[12] when analyzing the linear static and dynamic behavior of plates and plate structures. Lau and Hancock[13] have used the method to predict the buckling of plate structures, and Kwon and Hancock[14] have studied the nonlinear elastic response of some thin-walled structures. In all of these approaches, attention is limited to homogeneous materials, the analysis is in the context of CPT, and the type of finite strip used is the simplest one, which corresponds to the rather coarse assumption of linear variations of the in-plane components of displacement across the strip. To deal with the buckling and vibration of composite-laminated plate and shell structures, the present authors have developed the spline FSM in the contexts of both classical and first-order shear deformation theories.[15–20] A family of finite strip models has been generated, based on displacement fields that incorporate different polynomial degrees of crosswise representation and different degrees of longitudinal spline functions. This work has been further developed recently to include the postbuckling behavior of single composite laminated plates, of arbitrary lamination, in the contexts of CPT[21] and of SDPT.[22]

The present paper extends the spline FSM postbuckling analysis of Refs. 21 and 22 to embrace complicated prismatic plate structures (including also shell panels when treated as faceted structures). Again, the development takes place in the contexts of both CPT and of first-order SDPT, and arbitrary lamination is accommodated. The behavior is assumed to be geometrically nonlinear, and a total Lagrangian approach is used. The capability that has been developed has a quite general nature with regard to loading and to structure boundary conditions. Here, however, attention is restricted to the nonlinear response of structures that are subjected to progressive end shortening. The component plates of a model of a structure are assumed to be perfectly flat prior to loading.

Analysis

General Remarks

A typical prismatic plate structure of the type that is under consideration here is shown in Fig. 1. The structure of length A may have quite general boundary conditions at its longitudinal edges and at its ends, except that an applied progressive end shortening is specified. This end shortening, corresponding to a progressive uniform, end-shortening strain ε, may be applied in a particular horizontal plane that, for the structure of Fig. 1, is the plane containing PQ at a distance z^* from the middle surface of the main plate. Alternatively it may be applied to the complete end cross sections. The axes x', y', and z' (Fig. 1) are global axes, and the translational displacements u', v', and w' are corresponding global displacements.

As mentioned earlier, the analysis capability described here is developed in the contexts of both CPT and first-order SDPT. Attention will be concentrated on the SDPT analysis because the CPT approach is a fairly direct simplification of the SDPT approach.

Basis for SDPT Finite Strip Properties

Each component plate of a prismatic plate structure is modeled with one or more finite strips, which run the full length A of the structure. A typical finite strip in the SDPT context is shown in Fig. 2a wherein the indicated coordinates x, y, and z, middle surface displacements u, v, and w, and independent rotations ψ_x, ψ_y, and ψ_z are local quantities. Figure 2b shows an end view of the typical strip with its local system xyz aligned at an angle α to the global system $x'y'z'$. Note that the local rotation ψ_z has no role to play in the development of local strip properties, but is required for the transformation to the global system. In the global system, the rotations are $\psi_{x'}$, $\psi_{y'}$, and $\psi_{z'}$, as shown in Fig. 2b.

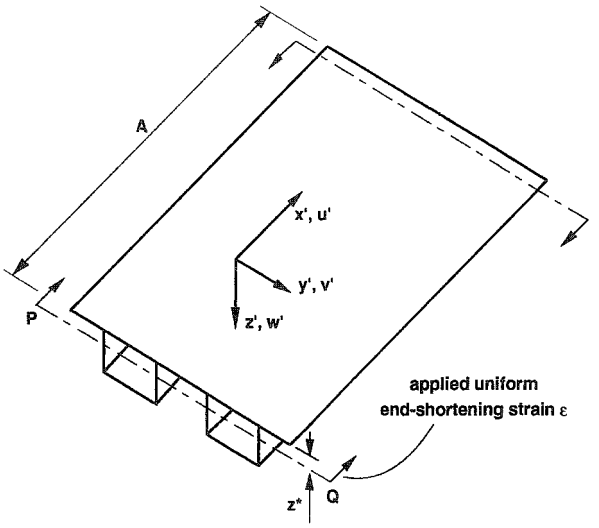

Fig. 1 Typical prismatic plate structure.

The strain–displacement relationships used here incorporate five strain components (at a general point). These are the in-plane nonlinear strains ε_x, ε_y, and γ_{xy} and the linear through-thickness shear strains γ_{yz} and γ_{zx}. The relationships, within the context of a total Lagrangian approach, are

$$\varepsilon = \begin{Bmatrix} \varepsilon_x \\ \varepsilon_y \\ \gamma_{yz} \\ \gamma_{zx} \\ \gamma_{xy} \end{Bmatrix} = \begin{Bmatrix} \dfrac{\partial u}{\partial x} + \dfrac{z\partial \psi_x}{\partial x} + \dfrac{1}{2}\left(\dfrac{\partial w}{\partial x}\right)^2 + \dfrac{1}{2}\left(\dfrac{\partial v}{\partial x}\right)^2 \\ \dfrac{\partial v}{\partial y} + \dfrac{z\partial \psi_y}{\partial y} + \dfrac{1}{2}\left(\dfrac{\partial w}{\partial y}\right)^2 + \dfrac{1}{2}\left(\dfrac{\partial v}{\partial y}\right)^2 \\ \dfrac{\partial w}{\partial y} + \psi_y \\ \dfrac{\partial w}{\partial x} + \psi_x \\ \dfrac{\partial u}{\partial y} + \dfrac{\partial v}{\partial x} + z\left(\dfrac{\partial \psi_x}{\partial y} + \dfrac{\partial \psi_y}{\partial x}\right) + \dfrac{\partial w}{\partial x}\dfrac{\partial w}{\partial y} + \dfrac{\partial v}{\partial x}\dfrac{\partial v}{\partial y} \end{Bmatrix} \tag{1}$$

The in-plane strain–displacement relationships are those that are obtained from Green's expressions for nonlinear strains[23] and using the basic assumptions of first-order SDPT for through-thickness variations of the three displacements [as in Eq. (1) of Ref. 22]. However, nonlinear terms in u have been neglected because they would be expected to have a very small effect, as have nonlinear terms that involve z. Note that nonlinear contributions in the crosswise displacement v are present in the expressions for ε_x, ε_y, and γ_{xy}. This allows consideration to be given to problems that exhibit post-overall-buckling response as well as to those that exhibit post-local-buckling response. In the latter situation the movement of junction lines may be small, and the nonlinear-v contributions would then have little effect and could be ignored, with consequent significant saving in solution time. In the former situation, however, the nonlinear-v contributions can have considerable significance on

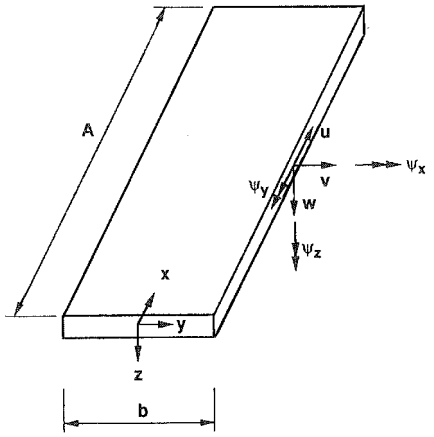

Fig. 2a SDPT finite strip.

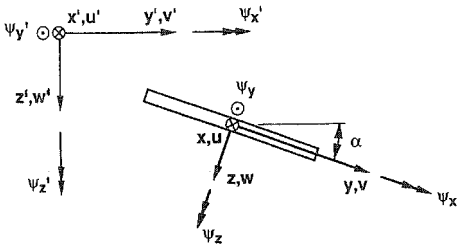

Fig. 2b Local and global systems.

accuracy of solution because the v and w displacements generally may be of similar magnitudes, where large movements of junction lines are involved.

In general, a component plate is a fiber-reinforced laminate composed of a number of bonded layers of unidirectional composite material. With the usual assumptions,[24] the stress–strain relationships at a general point for any layer are

$$\begin{Bmatrix} \sigma_x \\ \sigma_y \\ \tau_{yz} \\ \tau_{zx} \\ \tau_{xy} \end{Bmatrix} = \begin{bmatrix} Q_{11} & Q_{12} & 0 & 0 & Q_{16} \\ Q_{12} & Q_{22} & 0 & 0 & Q_{26} \\ 0 & 0 & Q_{44} & Q_{45} & 0 \\ 0 & 0 & Q_{45} & Q_{55} & 0 \\ Q_{16} & Q_{26} & 0 & 0 & Q_{66} \end{bmatrix} \begin{Bmatrix} \varepsilon_x \\ \varepsilon_y \\ \gamma_{yz} \\ \gamma_{zx} \\ \gamma_{xy} \end{Bmatrix}$$

$$\text{or} \quad \boldsymbol{\sigma} = \boldsymbol{Q}\boldsymbol{\varepsilon} \tag{2}$$

where Q_{rs}, $r, s = 1, 2, 6$, are plane-stress reduced stiffness coefficients and Q_{rs}, $r, s = 4, 5$, are through-thickness shear stress coefficients.

The constitutive equations for the laminate are obtained through use of Eqs. (1) and (2) and appropriate integration through the thickness. The equations are

where ε_x^*, ε_y^*, and γ_{xy}^* are middle-surface, in-plane strains, which are defined as are ε_x, ε_y, and γ_{xy}, respectively, in Eq. (1) except that the terms involving z are absent. N_x, N_y, and N_{xy} are the membrane direct and shearing forces per unit length, M_x, M_y, and M_{xy} are the bending and twisting moments per unit length, and Q_x and Q_y are through-thickness shear forces per unit length. The laminate stiffness coefficients are defined as

$$(A_{rs}, B_{rs}, D_{rs}) = \int_{-h/2}^{h/2} Q_{rs}(1, z, z^2)\, \mathrm{d}z, \qquad r, s = 1, 2, 6 \tag{4}$$

$$A_{rs} = k_r k_s \int_{-h/2}^{h/2} Q_{rs}\, \mathrm{d}z, \qquad r, s = 4, 5 \tag{5}$$

where the parameters $k_r k_s$ are shear correction factors that are determined in this study using the method of Whitney.[25]

Note that the constitutive equations allow for arbitrary lamination. Fully anisotropic behavior is accommodated, as is full coupling between in-plane and out-of-plane behaviors.

The strain energy density of an elastic body is $\boldsymbol{\sigma}^T\boldsymbol{\varepsilon}/2$. By the use of Eq. (2), the strain energy of a finite strip, U_p, can be expressed as

$$U_p = \frac{1}{2}\int_{V_e} \boldsymbol{\varepsilon}^T \boldsymbol{Q}\boldsymbol{\varepsilon}\, \mathrm{d}V_e \tag{6}$$

where V_e is the volume of the strip. Use of Eq. (1) in this expression and integration through the thickness with respect to z will give an expression for U_p as an integral over the strip middle-surface area of a function of the five fundamental displacement-type quantities, namely, u, v, w, ψ_x, and ψ_y. This complicated expression is not given here, but can be broken down into three distinct contributions that depend on quadratic, cubic, and quartic functions, namely, U_{p2}, U_{p3}, and U_{p4}, respectively, of the displacement-type quantities and their derivatives with respect to x and y. Thus,

$$U_p = U_{p2} + U_{p3} + U_{p4} \tag{7}$$

The nature of U_p is such that the problem is one of C^0-type continuity, that is, continuity across strip boundaries is required for each fundamental quantity, but not for any derivatives thereof. (Note that the specific definitions of the quadratic, cubic, and quartic strain energy contributions are given in Refs. 6 and 22 for the reduced situation in which the nonlinear-v contributions are excluded. In fact, the quadratic contribution is unchanged.)

SDPT Strip Displacement Fields and Models

In the SDPT spline FSM, the variation of each of the five fundamental quantities u, v, w, ψ_x, and ψ_y over the strip middle surface is represented basically as a summation of products of B-spline polynomial functions in the longitudinal x direction and interpolation functions in the crosswise y direction. However, extra terms may be present for u and v to represent a specific prescribed state of applied end-shortening strain.

$$\begin{Bmatrix} N_x \\ N_y \\ N_{xy} \\ M_x \\ M_y \\ M_{xy} \\ Q_y \\ Q_x \end{Bmatrix} = \int_{-h/2}^{h/2} \begin{Bmatrix} \sigma_x \\ \sigma_y \\ \tau_{xy} \\ z\sigma_x \\ z\sigma_y \\ z\tau_{xy} \\ \tau_{yz} \\ \tau_{zx} \end{Bmatrix} \mathrm{d}z = \begin{bmatrix} A_{11} & A_{12} & A_{16} & B_{11} & B_{12} & B_{16} & 0 & 0 \\ A_{12} & A_{22} & A_{26} & B_{12} & B_{22} & B_{26} & 0 & 0 \\ A_{16} & A_{26} & A_{66} & B_{16} & B_{26} & B_{66} & 0 & 0 \\ B_{11} & B_{12} & B_{16} & D_{11} & D_{12} & D_{16} & 0 & 0 \\ B_{12} & B_{22} & B_{26} & D_{12} & D_{22} & D_{26} & 0 & 0 \\ B_{16} & B_{26} & B_{66} & D_{16} & D_{26} & D_{66} & 0 & 0 \\ 0 & 0 & 0 & 0 & 0 & 0 & A_{44} & A_{45} \\ 0 & 0 & 0 & 0 & 0 & 0 & A_{45} & A_{55} \end{bmatrix} \begin{Bmatrix} \varepsilon_x^* \\ \varepsilon_y^* \\ \gamma_{xy}^* \\ \dfrac{\partial \psi_x}{\partial x} \\ \dfrac{\partial \psi_y}{\partial y} \\ \dfrac{\partial \psi_x}{\partial y} + \dfrac{\partial \psi_y}{\partial x} \\ \dfrac{\partial w}{\partial y} + \psi_y \\ \dfrac{\partial w}{\partial x} + \psi_x \end{Bmatrix} \tag{3}$$

In the longitudinal direction, the B-spline form of representation that is used is much the same as that utilized in earlier works by the authors[15–22] and described in detail in Ref. 26, and, hence, it is not necessary to give full details here. In employing the spline functions, the length A is divided into q sections, which are taken to be of equal length. In the crosswise direction, the interpolation functions used are the well-known Lagrangian functions.[15–22]

The displacement field of an SDPT spline finite strip is expressed as

$$\begin{Bmatrix} u \\ v \\ w \\ \psi_y \\ \psi_x \end{Bmatrix} = \begin{Bmatrix} u_p \\ v_p \\ 0 \\ 0 \\ 0 \end{Bmatrix} + \sum_{j=1}^{n+1} \begin{bmatrix} N_j & 0 & 0 & 0 & 0 \\ 0 & N_j & 0 & 0 & 0 \\ 0 & 0 & N_j & 0 & 0 \\ 0 & 0 & 0 & N_j & 0 \\ 0 & 0 & 0 & 0 & N_j \end{bmatrix} \times \begin{bmatrix} \bar{\Phi}_k & \mathbf{0} & \mathbf{0} & \mathbf{0} & \mathbf{0} \\ \mathbf{0} & \bar{\Phi}_k & \mathbf{0} & \mathbf{0} & \mathbf{0} \\ \mathbf{0} & \mathbf{0} & \bar{\Phi}_k & \mathbf{0} & \mathbf{0} \\ \mathbf{0} & \mathbf{0} & \mathbf{0} & \bar{\Phi}_k & \mathbf{0} \\ \mathbf{0} & \mathbf{0} & \mathbf{0} & \mathbf{0} & \bar{\Phi}_{k-1} \end{bmatrix} \begin{Bmatrix} \boldsymbol{d}^u \\ \boldsymbol{d}^v \\ \boldsymbol{d}^w \\ \boldsymbol{d}^{\psi_y} \\ \boldsymbol{d}^{\psi_x} \end{Bmatrix}_j \tag{8}$$

where the quantity j is the number of a reference line at which the strip degrees of freedom are located and there are $n+1$ reference lines across a strip, where n is the degree of polynomial representation (of each of the fundamental quantities) in the y direction. The $N_j(y)$ are the Lagrangian shape functions that define this representation, and of course, the definitions of the N_j vary with the choice of n. Here allowance is made for linear or quadratic or cubic representation, that is $n=1$ or 2 or 3. The three SDPT models are shown in end view in Fig. 3a, where M is the number of reference lines and indication is given of the type of freedom present at each line.

Concerning the longitudinal representation, $\bar{\Phi}_k(x)$ and $\bar{\Phi}_{k-1}(x)$ are modified B-spline function bases of degrees k and $k-1$, respectively. Note that a lower degree base is used in representing ψ_x than in representing w (or u, v, and ψ_y) to avoid possible shear-locking problems. The approach is referred to as a $B_{k,k-1}$-spline representation, and the value of k can be selected to be 2, 3, 4, or 5. The designation B_{32}-spline, for instance, indicates that modified B-spline function bases of degree 3, that is, cubic, are used in representing each of u, v, w, and ψ_y longitudinally while a modified basis of degree 2, that is, quadratic, is used in representing ψ_x. The $\boldsymbol{d}^u$, $\boldsymbol{d}^v$, $\boldsymbol{d}^w$, $\boldsymbol{d}^{\psi_y}$, and $\boldsymbol{d}^{\psi_x}$ are column matrices of generalized displacement parameters, or degrees of freedom, relating to u, v, w, ψ_y, and ψ_x, respectively. The series part of the displacement field of Eq. (8) is versatile with regard to the specification of basic boundary conditions. Kinematic conditions can be applied directly and explicitly by setting to zero any of the values of the fundamental quantities at a boundary, and natural conditions are properly allowed to be approached indirectly as a result of the application of the variational principle. This applies both at the structure ends and at the longitudinal edges.

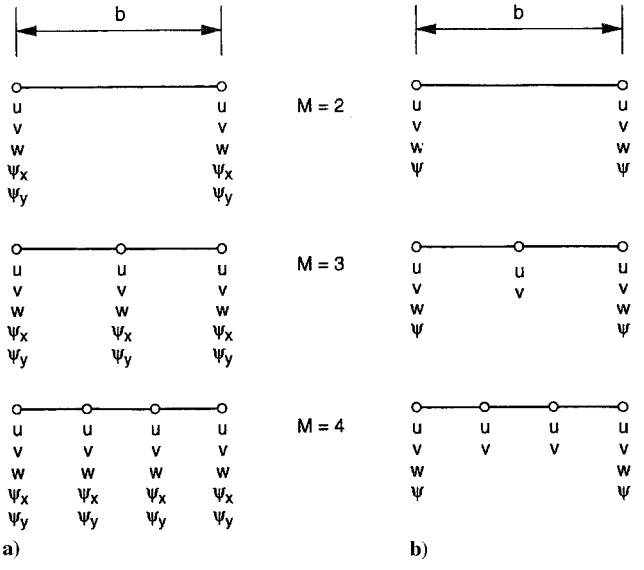

Fig. 3 Finite strip models for a) SDPT analysis and b) CPT analysis.

The extra part of the displacement field of Eq. (8) is that which involves u_p and v_p and will only be applied to any finite strip to which a progressive uniform end-shortening strain ε is applied. For such a strip, u_p and v_p are defined as

$$u_p = \varepsilon(A/2 - x), \qquad v_p = \varepsilon\beta y \tag{9}$$

This represents explicitly a progressive uniform end shortening, with the u_p term, and a possible Poisson expansion, through the v_p term, in a simple prebuckled state. If the strip ends are allowed free in-plane lateral expansion, in what is referred to as a type A problem,[5] then $\beta = \nu$, the Poisson's ratio, for isotropic material or $\beta = A_{12}/A_{22}$ for balanced orthotropic material. However, the presence of the v_p term is not essential or even particularly advantageous for the majority of type A problems involving structures (as distinct from single plates). If the plate ends are completely prevented from expanding laterally, in what is referred to as a type B problem,[5] then $\beta = 0$ anyway.

Stiffness Equations

The concern here is with the response of a plate structure to an applied progressive uniform shortening strain ε, perhaps at some specific geometric level. The potential energy of the end load associated with ε will be independent of the unprescribed degrees of freedom of the problem. Therefore, the total potential energy of a strip can in effect (so far as the minimization procedure is concerned) be equated to the strain energy U_p.

The strain energy of a finite strip can be determined as a function of all of the strip degrees of freedom $\boldsymbol{d}$, where the column matrix $\boldsymbol{d}$ includes $\boldsymbol{d}^u$, $\boldsymbol{d}^v$, $\boldsymbol{d}^w$, $\boldsymbol{d}^{\psi_y}$, and $\boldsymbol{d}^{\psi_x}$ at all reference lines j, on substituting the chosen displacement field of Eq. (8) into Eq. (7). This strip strain energy, as a function of the unprescribed freedoms, can be expressed eventually in the form (where a further term, which is proportional to ε^2, has been excluded from consideration because it is independent of the unprescribed freedoms):

$$U_p = -\varepsilon \boldsymbol{d}^T \boldsymbol{V} + \tfrac{1}{2}\boldsymbol{d}^T(\boldsymbol{K} - \varepsilon \boldsymbol{K}^*)\boldsymbol{d} + \tfrac{1}{6}\boldsymbol{d}^T \boldsymbol{K}_1 \boldsymbol{d} + \tfrac{1}{12}\boldsymbol{d}^T \boldsymbol{K}_2 \boldsymbol{d} \tag{10}$$

where $\boldsymbol{K}, \boldsymbol{K}_1, \boldsymbol{K}_2$ and $\boldsymbol{K}^*$ are square symmetric stiffness matrices. The individual entries of $\boldsymbol{K}$ and $\boldsymbol{K}^*$ are constants, whereas those of $\boldsymbol{K}_1$ and $\boldsymbol{K}_2$ are linear and quadratic functions, respectively, of the freedoms. Hence the second, third, and fourth quantities on the right-hand side of Eq. (10) represent energy terms that are quadratic, cubic, and quartic functions, respectively, of the freedoms. The first quantity on the right-hand side, in which $\boldsymbol{V}$ is a column matrix of constants, is a linear function of the freedoms. This linear function is present at this stage, when dealing directly in terms of degrees of freedom rather than with the fundamental displacement-type quantities themselves, simply because the fundamental quantities are expressed in terms of both degrees of freedom and of ε, as in Eqs. (8) and (9).

Many integrations are required in evaluating the energy. Integrations across a strip, in the y direction, are determined in standard fashion using Gauss quadrature, with seven points across a strip. Along a strip, in the x direction, there is the need to perform integrations of polynominal spline functions, and derivatives thereof, and of double, triple, and quadruple products of such functions and derivatives. It is most important, so far as efficiency is concerned, that these integrations be determined in a manner that takes account of the repetitive nature of the local spline functions. This is achieved so that the integrations are evaluated numerically and need only be determined once, outside of any iteration cycle.

The preceding energy expression for the individual finite strip is written in terms of local quantities. Before assembling the energy of a complete structure, it is necessary to transform from the local xyz configuration to the global $x'y'z'$ configuration. To do this, it is required to introduce at the local level a third component of rotation, namely, ψ_z, the rotation about the local z axis. At the local level such introduction is artificial in the sense that no contributions to the strip

matrices are associated with it, that is, the strip matrices are simply expanded in size by appropriate addition of rows and columns of zeros. The procedure is necessary, however, because in the global system there are indeed three significant components of rotation, namely, $\psi_{x'}$, $\psi_{y'}$, and $\psi_{z'}$. For each reference line and each series term, the transformation has the form

$$\begin{Bmatrix} u \\ v \\ w \\ \psi_y \\ \psi_x \\ \psi_z \end{Bmatrix} = \begin{bmatrix} 1 & 0 & 0 & 0 & 0 & 0 \\ 0 & \cos\alpha & \sin\alpha & 0 & 0 & 0 \\ 0 & -\sin\alpha & \cos\alpha & 0 & 0 & 0 \\ 0 & 0 & 0 & 1 & 0 & 0 \\ 0 & 0 & 0 & 0 & \cos\alpha & \sin\alpha \\ 0 & 0 & 0 & 0 & -\sin\alpha & \cos\alpha \end{bmatrix} \begin{Bmatrix} u' \\ v' \\ w' \\ \psi_{y'} \\ \psi_{x'} \\ \psi_{z'} \end{Bmatrix} \tag{11}$$

where α is the angle shown in Fig. 2b.

After the required transformations have been made, the total energy of a complete structure is simply the summation of the energies of all of the individual finite strips. Correspondingly, structure matrices are generated by appropriate summation of strip matrices, and following the application of prescribed kinematic boundary conditions, the total strain energy can be expressed in a similar form to that of Eq. (10) as

$$\bar{U}_p = -\varepsilon \bar{\boldsymbol{d}}^T \bar{\boldsymbol{V}} + \tfrac{1}{2}\bar{\boldsymbol{d}}^T(\bar{\boldsymbol{K}} - \varepsilon \bar{\boldsymbol{K}}^*)\bar{\boldsymbol{d}} + \tfrac{1}{6}\bar{\boldsymbol{d}}^T \bar{\boldsymbol{K}}_1 \boldsymbol{d} + \tfrac{1}{12}\bar{\boldsymbol{d}}^T \bar{\boldsymbol{K}}_2 \bar{\boldsymbol{d}} \tag{12}$$

where now an overbar indicates a structure quantity.

The set of nonlinear structure equilibrium equations corresponding to a specified value of ε can then be obtained by applying the minimization principle and has the form[5]

$$-\varepsilon \bar{\boldsymbol{V}} + \left(\bar{\boldsymbol{K}} - \varepsilon \bar{\boldsymbol{K}}^* + \tfrac{1}{2}\bar{\boldsymbol{K}}_1 + \tfrac{1}{3}\bar{\boldsymbol{K}}_2\right)\bar{\boldsymbol{d}} = \boldsymbol{0} \tag{13}$$

where the stiffness matrices $\bar{\boldsymbol{K}}$, $\bar{\boldsymbol{K}}^*$, $\bar{\boldsymbol{K}}_1$, and $\bar{\boldsymbol{K}}_2$ are duplicated from Eq. (12) as a direct consequence of the variational procedure, just as in standard finite element formulations (for example, see Ref. 27).

These equations are solved for $\bar{\boldsymbol{d}}$ using the well-known Newton–Raphson iterative method in which use is made of the tangent stiffness matrix $\bar{\boldsymbol{K}}_T$, which has the definition[5]

$$\bar{\boldsymbol{K}}_T = \bar{\boldsymbol{K}} - \varepsilon \bar{\boldsymbol{K}}^* + \bar{\boldsymbol{K}}_1 + \bar{\boldsymbol{K}}_2 \tag{14}$$

When the values of the degrees of freedom have been found, at a specified value of ε, the fundamental quantities can be calculated at any point in any finite strip using Eq. (8), and force and moment quantities can then be calculated using Eq. (3). One quantity of interest is the average longitudinal force N_{av} acting on a structure at a given applied strain. This is determined by a procedure involving the summation of forces acting on the individual strips. Thus,

$$N_{\text{av}} = \sum \int_{-b/2}^{b/2} \int_0^A \frac{N_x(x, y)}{A} \, \mathrm{d}x \, \mathrm{d}y \tag{15}$$

CPT Finite Strip Analysis

The preceding SDPT approach can be simplified to a CPT approach by adopting the Kirchhoff normalcy condition. Then the rotations ψ_x and ψ_y of the SDPT theory are no longer independent quantities but are directly dependent on the deflection w through the equations

$$\psi_x = -\frac{\partial w}{\partial x}, \qquad \psi_y = -\frac{\partial w}{\partial y} \tag{16}$$

It follows that in the CPT analysis the through-thickness shear strains γ_{yz} and γ_{zx} vanish [see Eq. (1)] and that the corresponding stresses τ_{yz} and τ_{zx}, shear stiffness coefficients A_{44}, A_{45}, and A_{55}, and shear forces Q_x and Q_y can be ignored [in Eqs. (2), (3), and (5)]. It also means that, in the local configuration, the CPT strip behavior is governed by only three fundamental middle-surface quantities, namely, the translational displacements u, v, and w. The strain energy U_p [Eqs. (6) and (7)] now contains second derivatives of w, and it follows that C^1-type continuity is required for w, that is, continuity of both w and $\partial w/\partial y$ is required at strip edges.

The displacement field for CPT-based strip models is given by a reduced form of Eq. (8) as

$$\begin{Bmatrix} u \\ v \\ w \end{Bmatrix} = \begin{Bmatrix} u_p \\ v_p \\ 0 \end{Bmatrix} + \sum_j \begin{bmatrix} N_j & 0 & 0 \\ 0 & N_j & 0 \\ 0 & 0 & N_{jH} \end{bmatrix} \begin{bmatrix} \bar{\Phi}_k & \boldsymbol{0} & \boldsymbol{0} \\ \boldsymbol{0} & \bar{\Phi}_k & \boldsymbol{0} \\ \boldsymbol{0} & \boldsymbol{0} & \bar{\Phi}_k \end{bmatrix} \begin{Bmatrix} \boldsymbol{d}^u \\ \boldsymbol{d}^v \\ \boldsymbol{d}^w \end{Bmatrix}_j \tag{17}$$

The crosswise representation of u and v is exactly as in the SDPT analysis: the $N_j(y)$ are Lagrangian shape functions and the upper limit of the indicated summation on j is $n + 1$. The crosswise representation of w is now rather different than in the SDPT analysis, to take account of the C^1-type continuity requirement. The N_{jH} are cubic Hermitian shape functions, and the upper limit of the summation is 4, but the freedoms correspond to values of w and ψ ($=\partial w/\partial y$) at the two strip edges. Three CPT strip models are created, each having cubic (Hermitian) variation of w crosswise, but with either linear, quadratic, or cubic (Lagrangian) variation of u and v crosswise, that is, $n = 1$, 2, or 3. The three CPT models are shown in end view in Fig. 3b. In the longitudinal direction, each of u, v, and w is represented by modified B-spline function bases of degree k. The approach is referred to as a B_k-spline representation, and k can be selected here to be 2, 3, 4, or 5. The designation B_3-spline, for instance, indicates that a modified B-spline function basis of degree 3, that is, cubic, is used in representing each of u, v, and w longitudinally.

The remaining procedures in the CPT analysis are very similar to those of the SDPT analysis. Further discussion will not be given here, except to note that in the transformation relationship given in Eq. (11) the only rotation present in the CPT analysis is $\psi_y = \psi_{y'}$.

Applications

Preamble

The analysis capability described has, of course, been used as the basis for the development of a computer software package. Results generated using this package are presented for several problems involving the nonlinear elastic response of prismatic structures subjected to progressive end shortening. The emphasis in this study is in predicting general response characteristics, such as end load-shortening strain histories and the development of deformation patterns, and in comparing such predictions with alternative analytical predictions and with test results where applicable. Detailed stress results are not considered.

Although a variety of finite strip models is available in the developed capability, all of the applications considered here are based on the use of one particular model in the contexts of each of SDPT and CPT analyses. In the context of SDPT, the model used is that corresponding to $M = 3$ in Fig. 3a, that is, quadratic Lagrangian interpolation across the strip, and to B_{32}-spline representation longitudinally. In the context of CPT analysis, the model used is that corresponding to $M = 3$ in Fig. 3b, that is, quadratic Lagrangian interpolation for u and v, and cubic Hermitain interpolation for w across the strip, and to B_3-spline representation longitudinally.

The strip models used here have been used earlier[21,22] in studies of the postbuckling response of single rectangular plates. The characteristics of these models, and others of the same family and of related semi-analytical FSM (or S-a FSM) models, have been well established with regard to the convergence of results with respect to the number of spline sections q used and to the number of strips NS used (for example, see Refs. 5, 6, 9, 10, 16–21, and 28). Hence, with one exception, convergence studies are not reported here, and results are given for just a specified single value of q and of NS in each application. Of course, the values used for q and NS are those that are judged to be sufficient to represent accurately the structural response, the complexity of which varies considerably with the application. Broadly speaking, at least two spline sections are used per

longitudinal half-wavelength, and two or more strips are used per crosswise half-wavelength.

Orthotropic Box Column

The structure considered is an orthotropic box column of square cross section, whose overall length is A, component plate thickness is h, and component plate width (between centerlines of component plates) is B. The geometry is such that $A/B=3$ and $B/h=20$. The component plates are 0/90/0/90/0 five-layer, cross-ply laminates, with fiber angles in degrees and with each 0-deg layer of thickness $h/6$ and each 90-deg layer of thickness $h/4$. The material properties of each layer are $E_L/E_T=30$, $G_{LT}/E_T=0.6$, $G_{TT}/E_T=0.5$, and $\nu_{LT}=0.25$, where the symbols have their standard meaning.

The box column is assumed to be supported by diaphragms at both of its ends, so that at $x=0, A$ the kinematic conditions in the planes of the ends, in terms of local displacements, are those of a type B problem, that is, $v=w=\psi_y=0$. Furthermore the column is subjected to a progressive uniform end shortening, over the whole cross section, such that at $x=0, A$ we also have $u=\pm A\varepsilon/2$, where ε is the end-shortening strain. Thus, in total, the column is assumed to be compressed along its length between rigid, frictional platens.

The problem considered has been studied earlier by Dawe et al.[9] when using both a developed semi-analytical FSM and an FEM approach using the LUSAS general purpose software package. It is known that initial buckling occurs in a local mode having three longitudinal half-waves and that postbuckling behavior has a similar local character. The S-a FSM approach of Ref. 9 is, in fact, based directly on the consideration of local behavior by adopting certain simplifying assumptions and considering an analysis length equal to one half-wavelength of the response, that is, $A/3$. The results from this approach compare closely with those of the LUSAS FEM approach, which are not restricted to consideration of one half-wavelength.

In applying the present spline FSM approach to the problem, the full structure length is modeled, that is, the finite strips are of length A, and nine spline sections are used along the length, that is $q=9$. Because of the double symmetry of the problem, with regard to the two centroidal axes of the box cross section, it is only necessary to model a quadrant of the cross section. This is done by the use of 10 identical finite strips of width $B/10$. Analysis is conducted in the contexts of both CPT and SDPT.

The FEM results of Ref. 9 are used again here for comparison purposes. These LUSAS results are based on the use of a mesh of 72 elements in one-eighth of the box structure because three planes of symmetry exist: three elements are used across each of the two half-plates forming a symmetric quadrant of the box cross section, and 12 elements are used along a symmetric half-length $A/2$ of the structure. The elements used are designated QSL8 and are eight-node semiloof shell elements, with 32 degrees of freedom, which are classified as thin elements because through-thickness shearing effects are largely excluded. The LUSAS default rule of five-point numerical integration is used in evaluating element properties. In obtaining the nonlinear solution, a total Lagrangian formulation is used in conjunction with the full nonlinear strain–displacement equations.

The spline FSM predictions of the nonlinear response of the box column to progressive end shortening, together with the comparative FEM predictions, are shown in Fig. 4a (average stress σ_{av} vs shortening strain ε) and Fig. 4b (maximum deflection w_{max} vs ε). Note that in the FEM predictions σ_{av} is calculated as the straight average of values of σ_x at all nodes of the structural model.

It can be seen from Fig. 4 that there is a quite significant difference between the two sets of FSM results, in the contexts of CPT and SDPT, and hence that the effects of through-thickness shearing action are not negligible in this application. It can also be seen that the LUSAS FEM results provide verification of the validity of the developed spline FSM approach.

Orthotropic, Two-Blade Stiffened Panel

The cross section of the rectangular panel under consideration here is shown in Fig. 5 (wherein the depth of the stiffeners, i.e., 80 mm, is measured from the middle plane of the main plate). The panel length is $A=2000$ mm. The main plate and the stiffeners are five-layer, orthotropic laminates of precisely the same type as defined in the earlier application but now with the added specification that $E_T=13$ GN/m^2.

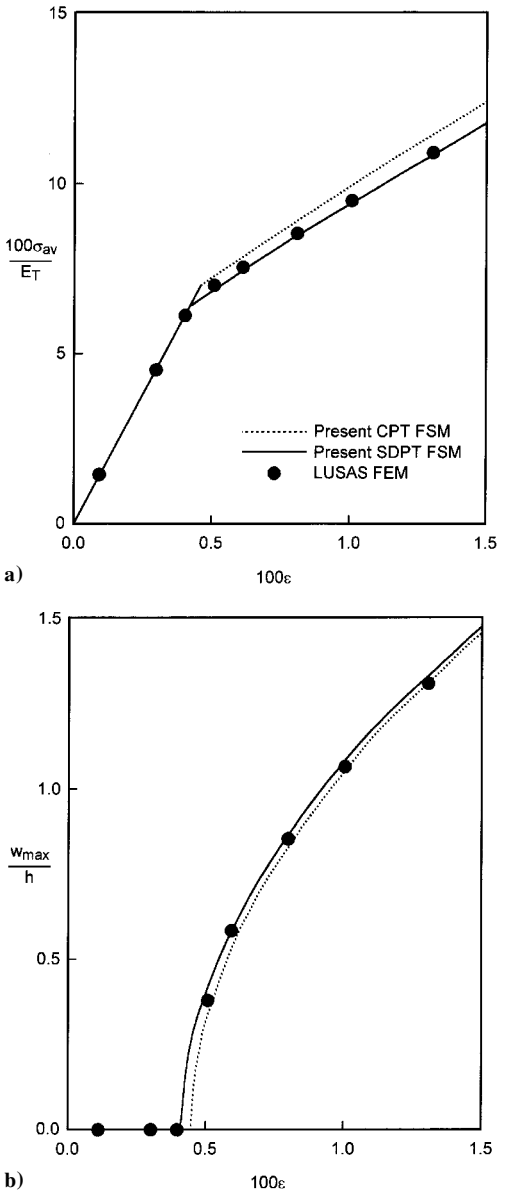

Fig. 4 Nonlinear response of the orthotropic box to applied shortening strain: variation of a) average longitudinal stress and b) maximum deflection.

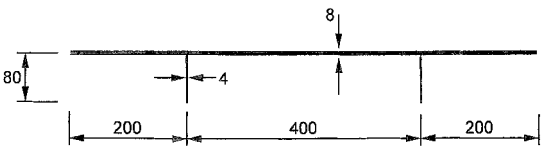

Fig. 5 Cross section of the two-blade stiffened panel. (Dimensions are in millimeters.)

The main plate is assumed to be subjected to a progressive uniform end shortening while the stiffeners are free to expand or contract longitudinally, and hence the structure ends are free to rotate about the y axis in a manner consistent with simple supports. Specifically, in the context of CPT and in terms of local displacements, the prescribed end conditions on the whole cross section are that $v=w=0$, with the extra condition on the main plate, only, being that $u=\pm A\varepsilon/2$ at $x=0, A$. The longitudinal edges of the main plate are simply supported for out-of-plane behavior, that is, $w=0$, but are free to move in-plane.

Again, the problem considered has been studied earlier, by the authors,[10] when using a semi-analytical FSM developed for the analysis of post-overall-buckling behavior and when also utilizing the

Table 1 FSM values of F and w_c at $\varepsilon = 0.05\%$ for the orthotropic, two-blade stiffened panel

Solution method	Number of strips NS	Number of longitudinal sections q or terms r				
		1	2	3	4	5
				F, kN		
Spline FSM	3	632.4	620.4	620.1	620.0	619.9
S-a FSM[10]	3	642.8	622.0	620.2	620.0	——
	5	642.5	621.0	619.4	619.1	——
	10	——	620.8	——	——	——
				w_c, mm		
Spline FSM	3	7.397	8.484	8.493	8.412	8.413
S-a FSM[10]	3	6.822	8.420	8.416	8.427	——
	5	6.838	8.475	8.472	8.482	——
	10	——	8.481	——	——	——

LUSAS FEM package for purposes of comparison. The response of the panel is indeed of the overall type and is of a continuously progressive nature with no bifurcational buckling as such.

In applying the present spline FSM, in the context of CPT alone, a symmetric (about the longitudinal centerline) half of the structure is modeled with only three strips of length A, one in a stiffener and one on either side of it in the half of the main plate. For this simple crosswise modeling, a convergence study has been conducted with an increasing number of spline sections for values of end force F (over the full panel width) and of central deflection w_c at the particular value of end-shortening strain of 0.05%. The results are shown in Table 1 together with results obtained earlier[10] when using the S-a FSM. In the latter case, the crosswise modeling is varied, with 3 strips (1 in the stiffener, 1 either side of it), 5 strips (1, 2), and 10 strips (2, 4) used in turn, and with different numbers of terms, r, used in the series representation of the longitudinal variation of displacements. The two sets of results show a very close comparison and confirm that the very simple crosswise modeling adopted in using the spline FSM is sufficient in this application in which the deformed shape of the panel is quite simple, that is, not local.

The overall response of the structure to progressive end shortening of the main plate, as predicted by the spline FSM ($q = 5$) and by LUSAS FEM (using a mesh of 70 QSL8 elements in a symmetric quadrant of the structure), is shown in Fig. 6a (F vs ε) and Fig. 6b (w_c vs ε). Close agreement between the results of the two approaches is evidenced. Note that the present spline FSM response curves in Figs. 6 are virtually identical with the corresponding curves generated for the S-a FSM and shown in Fig. 8 of Ref. 10.

Isotropic, Six-Blade Stiffened Panel

The cross section of this panel is shown in Fig. 7. The panel length is $A = 762$ mm, and hence the panel is square in plan. Here the panel is not of composite-laminated construction but is made of aluminium, with Young's modulus $E = 72.4$ GN/m^2 and Poisson's ratio $\nu = 0.32$. Because the geometry is thin, and the material is metallic, analysis will be conducted in the context of CPT.

The panel is one of seven panels considered in a detailed finite element buckling study by Stroud et al.[28] and later also considered by Peshkam and Dawe[29] when using the S-a FSM to predict buckling loads. In these buckling studies, the panels are assumed to have ends that are diaphragm supported (with $v = w = 0$) and longitudinal edges that are simply supported ($w = 0$), and to be subjected to combinations of shear loading and compressive longitudinal loading. In the present study, the panel referred to as NASA example 4 is considered, and this is defined earlier and shown in Fig. 7. The loading case of interest in the buckling studies is that of a pure compressive loading based on the assumption of uniform longitudinal prebuckling strain. The bifurcational buckling load is calculated as 39.47 kN using the S-a FSM, whereas the calculated FEM value is just 0.24% higher. The corresponding buckled mode shape is a local one, with six longitudinal half-waves.

The postbuckling behavior of the NASA example 4 panel under progressive uniform end shortening has been considered by Dawe et al.[9] using the S-a FSM. However, in this earlier approach the simplified local analysis is used, incorporating assumptions that allow the analysis to be performed over only a specified half-wavelength

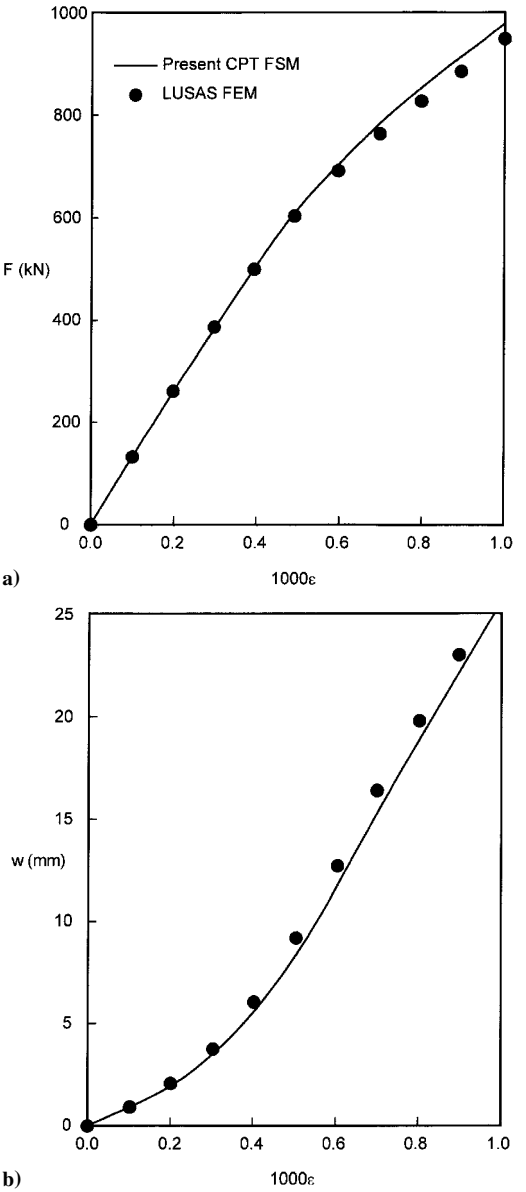

Fig. 6 Nonlinear response of the two-blade stiffened panel to applied shortening strain: variation of a) end force and b) central deflection.

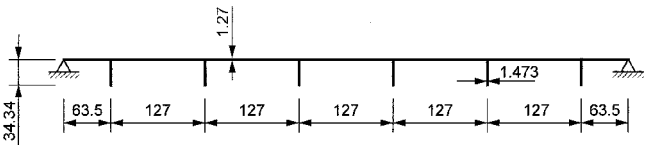

Fig. 7 Cross section of the six-blade stiffened panel. (Dimensions are in millimeters.)

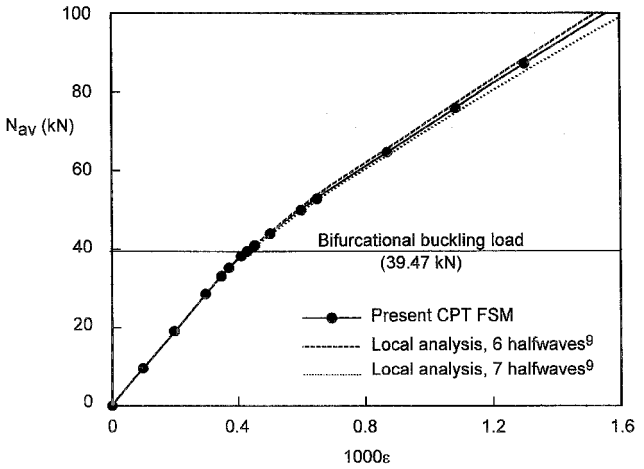

Fig. 8 Nonlinear response of the six-blade stiffened panel: variation of average longitudinal force with applied shortening strain.

rather than over the whole panel. In fact, because the bifurcational buckling load corresponding to seven longitudinal half-waves was found to be close to that corresponding to six half-waves, two separate analyses were performed for these two distinct numbers of half-waves. It was revealed that, in the context of the local analyses, buckling and initial postbuckling corresponds to six longitudinal half-waves but that at a fairly early stage of postbuckling there is a change to seven half-waves.

In the present nonlinear spline FSM study, the approach is much more general than in the earlier study[9] because now the full length of the structure is considered, with no preconception of any likely longitudinal form of the buckling or postbuckling response. The panel is assumed to be subjected to progressive uniform end shortening over the whole cross section, and the prescribed end conditions, in terms of local displacements, are that at $x = 0$, A we have $u = \pm A\varepsilon/2$ and $w = 0$, $v \neq 0$, that is, the component plates are simply supported for out-of-plane behavior and are free to expand in their planes. The longitudinal edges of the main plate are simply supported for out-of-plane behavior, that is, $w = 0$, but are free to move in-plane. The FSM model takes note of the symmetry of the response about the longitudinal center line and uses nine strips across half the panel width (one for each of the three stiffeners and six of equal width for half of the main plate), just as in the earlier study.[9] Along the length A of the structure, 16 spline sections are used.

The general response of the panel (N_{av} vs ε) as predicted by the present spline FSM approach is shown in Fig. 8 together with the predictions of the restricted earlier S-a FSM approach, which correspond to the two prescribed values ($A/6$ and $A/7$) of half-wavelength. It is seen that there is a close comparison between the two approaches, and this obviously helps to prove the validity of both the present spline FSM approach and of the earlier local S-a FSM. Note that in the present approach there is no bifurcational buckling as such (unlike in the earlier approach), but, rather, a continuous progressive change throughout the deformation process. However, the knee of the curve in Fig. 8 is quite sharp and relates closely to the value of bifurcational buckling force of 39.47 kN predicted in Ref. 28.

The progressive buildup of deformation in the panel, as predicted by the present approach, is illustrated for six particular values of shortening strain in Fig. 9. The views shown are of the modeled symmetric half-panel, from the stiffener side. It can be seen that at a low value of strain there is some deformation of an overall type, followed by local deformation with six longitudinal half-waves in the region of the theoretical buckling load, and then by the formation of seven half-waves at higher values of strain.

Three-Blade Stiffened Curved Panel

Snell and Greaves[30] have considered the buckling and postbuckling under progressive uniform end shortening of a number of blade-stiffened curved panels made of carbon fiber-reinforced plastic and provide details of experimental work into the advanced postbuckled

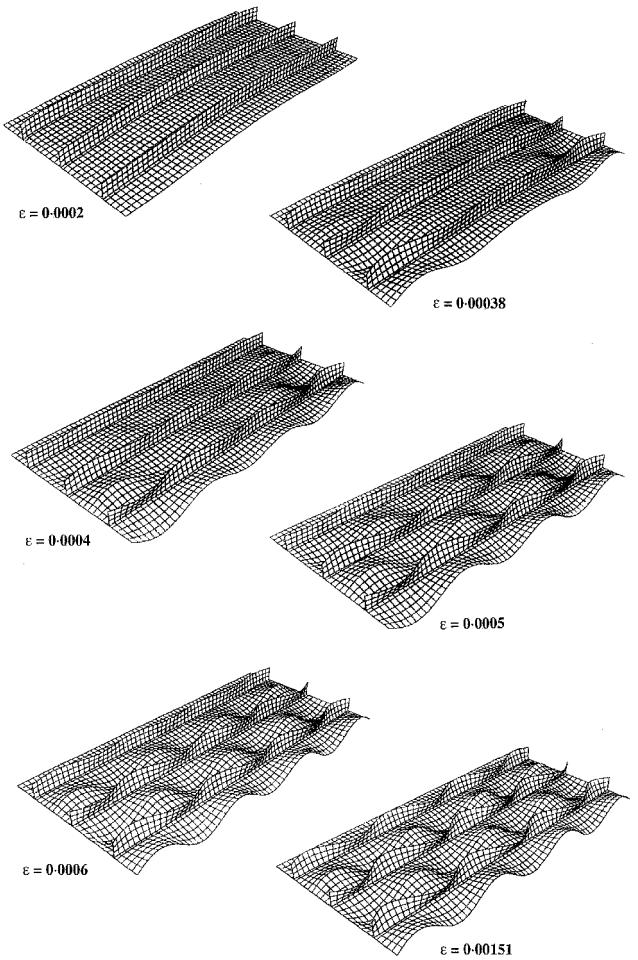

Fig. 9 Deformed shapes of one-half of the six-blade stiffened panel at six applied strain levels.

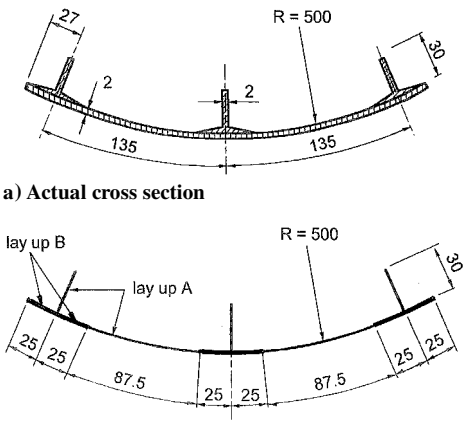

a) Actual cross section

b) Modeled cross section

Fig. 10 Blade-stiffened curved panel.

regime. The results presented by Snell and Greaves for one particular curved panel are used for comparison purposes with results generated using the present FSM capability. This panel is stiffened by three blade stringers, and its actual cross section is shown in Fig. 10a.[30] The panel has a length of 540 mm. The ends of the panel are fully clamped against any movement, except for the uniform end shortening $u = \pm A\varepsilon/2$ over the whole cross section. The two external longitudinal edges of the panel are completely free.

The bifurcational buckling of this panel has been analyzed in Ref. 29 and again later by the present authors when using the PASSAS software package,[20] which utilizes the spline FSM in predicting buckling loads of both flat plate and curved shell structures. The cross-sectional modeling used in the analysis is shown

in Fig. 10b, with the ply dropoff regions of the actual structure, where the stringers are bonded to the skin, replaced by a slightly thicker area of skin of uniform thickness. The nominal ply thickness is 0.125 mm and the material properties are assumed to be $E_L = 130$ GN/m^2, $E_T = 10$ GN/m^2, $G_{LT} = G_{TT} = 6$ GN/m^2, and $\nu_{LT} = 0.3$.

In the analysis model the balanced layup details are (see Fig. 10b) layup A, $[+45/0/-45/0]_{2s}$, with total thickness 2 mm and layup B, $[+45/0/(+45/0/-45/0)_2]_s$, with total thickness 2.5 mm.

By the use of a very fine crosswise modeling, with the curved skin represented by curved finite strips, with a total of 714 strips used in the whole cross section, and with $q = 12$, the linear bifurcational buckling load has been calculated as 109.9 kN in the context of first-order shear deformation theory.[20] The corresponding experimental buckling load[30] is 107 kN for the panel designated B1S31 in the work of Snell and Greaves.[30] (In fact, three nominally identical panels of the type described here were tested and different buckling loads were measured, but the 107-kN value seems to be the most reliable result, reflecting the least influence of initial imperfection.)

When using the present FSM capability to predict the nonlinear response of the subject panel to progressive end shortening, the crosswise modeling is restricted to the use of flat strips. The curved skin is represented in faceted fashion with the external reference lines of each flat strip lying on the curved middle surface of the skin. Of course, this faceted representation introduces an extra modeling error, but its effect should not be large in this problem so long as a reasonable number of strips is used. In fact, 26 strips of equal width are used in modeling the curved skin, with one strip used in modeling each of the three stiffeners, that is, $NS = 29$. The analysis is conducted in the context of SDPT and $q = 10$.

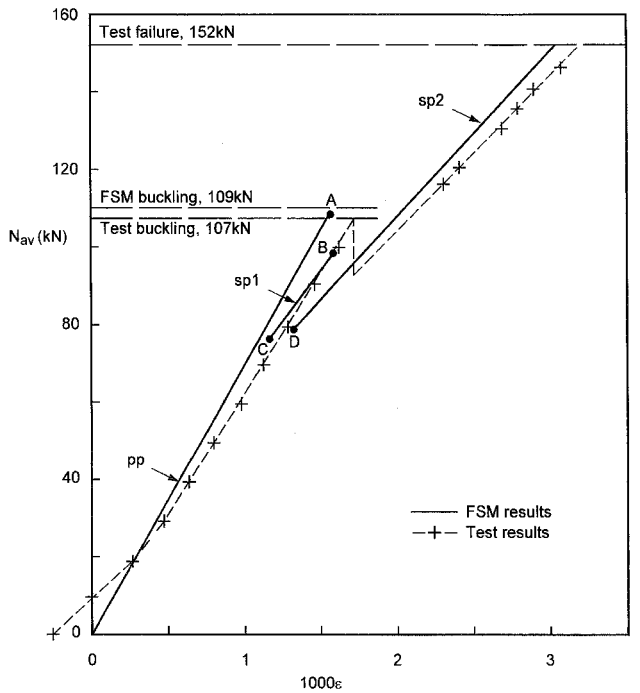

Fig. 11 Nonlinear response of the blade-stiffened curved panel: variation of average longitudinal force with applied shortening strain.

The general response of the panel (N_{av} vs ε) to progressive end shortening as predicted by the spline FSM approach is shown in Fig. 11, together with the experimental results.[30] The FSM predictions reveal a complicated response with a primary path (pp), a secondary path 1 (sp1), and a secondary path 2 (sp2). The predicted pp is stable with increasing end shortening up to point A (of Fig. 11) and is unstable thereafter. Any attempt to proceed beyond A on path pp results in the response dropping to sp1, corresponding to a lower value of N_{av}. This path can be traced back to point C, and is stable between B and C, but becomes unstable above B when response drops to sp2. This path is stable in going back to point D (below which it becomes unstable) and is always stable going forward from D with increasing ε. It is the only stable path for values of ε above about 0.00158. The deformed configurations of the panel in the three paths, at particular values of shortening strain, are shown in Fig. 12. On sp2, the main body of the panel, that is, the region within the outer two stiffeners, is seen to have two half-waves both along and across the panel.

The experimental results presented graphically in Ref. 30 reveal what is taken to be an initial bedding in phase, during which any slack in the testing machine and systems is taken up. This occurs at low values of loading (below about 30 kN) when the panel response is nonlinear, before the response becomes effectively linear, as expected, along the main part of the primary path. In showing these experimental results here in Fig. 11, an adjustment has been made by moving the set of results horizontally by a particular amount of strain such that when the linear part of the pp is projected it goes through the N_{av}/ε origin.

Given the complexity of the response in this problem, a close comparison of the experimental results with the FSM predictions is revealed in Fig. 11, although the longitudinal stiffness of the FSM model is somewhat greater than the experimental stiffness on the pp. (This may perhaps be because of variations in the initial curvature of the test panel over its surface, because of manufacturing difficulties, and/or because the material properties quoted in Ref. 30 and used here are assumed, rather than measured, and are not an accurate reflection of the properties of the actual panel.) The basic features of the nonlinear response predicted using the FSM are present in the test results, including in particular the unstable drop in load in moving from the primary path to a secondary path. It is remarked in Ref. 30 that the final experimental buckled mode has "two half waves in both the axial and circumferential directions, seen as a single dominant inward buckle in each bay." This description fits very well the deformed shape predicted for sp2 by the finite strip approach, shown in Fig. 12. Finally, note that in the experiment[30] the panel is deemed to have failed at a relatively low load of 152 kN (and a low strain of a little over 0.3%) due to delamination of the outer stringers and that the predicted sp2 deformed shape (Fig. 12) does show severe curvature in regions of these stringers.

Curved Panel with Edge Stiffeners

The final example concerns another composite-laminated, curved panel for which details have been made available to the authors by private communication from the Defence Evaluation and Research Agency (DERA) Farnborough. The cross section of the edge-stiffened panel is shown in Fig. 13a. The length of the panel is 460 mm. The ply thickness is again 0.125 mm, with a balanced 32-ply layup of $[45/-45/0/90/-45/45/0/0/45/-45/0/0/-45/45/90/90]_s$ construction. The ply material properties are $E_L =$

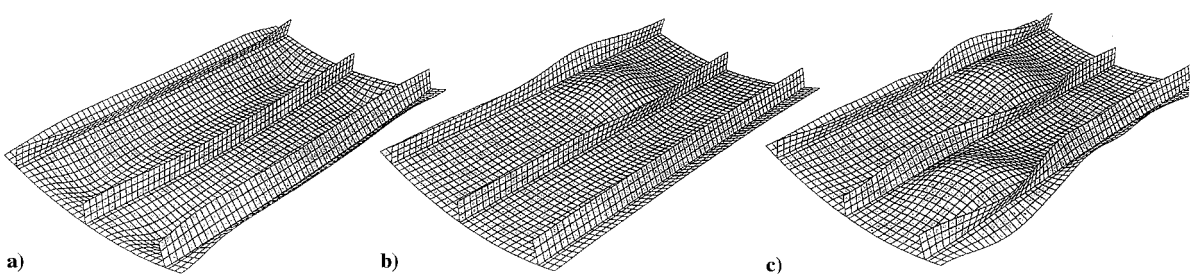

Fig. 12 Deformed shapes of the blade-stiffened curved panel: a) on pp, b) on sp1, and c) on sp2.

135 GN/n^2, $E_T = 9.2$ GN/m^2, $G_{LT} = G_{TT} = 5.4$ GN/m^2, and $\nu_{LT} = 0.28$.

The physical panel has been tested at DERA Farnborough by applying a progressive uniform end shortening to the panel up to beyond the buckling level. As in the preceding example, in the test the longitudinal edges of the panel were completely free and the curved ends were notionally fully clamped. The only test information available is that the buckling load was 880 kN and that the postbuckled shape of the panel was as shown in Fig. 13b.

In the study of the response of this panel using the spline FSM in the context of first-order shear deformation theory, a linear bifurcational buckling analysis was first performed using the PASSAS program[19,20] with a model having 80 flat and curved finite strips,

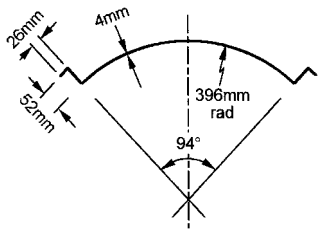

a) Cross section

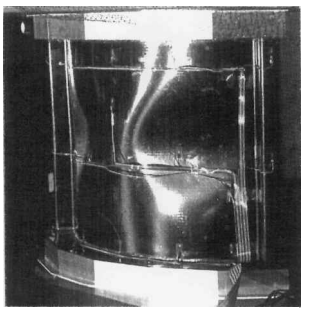

b) Experimental deformed shape

Fig. 13 Curved panel with edge stiffeners.

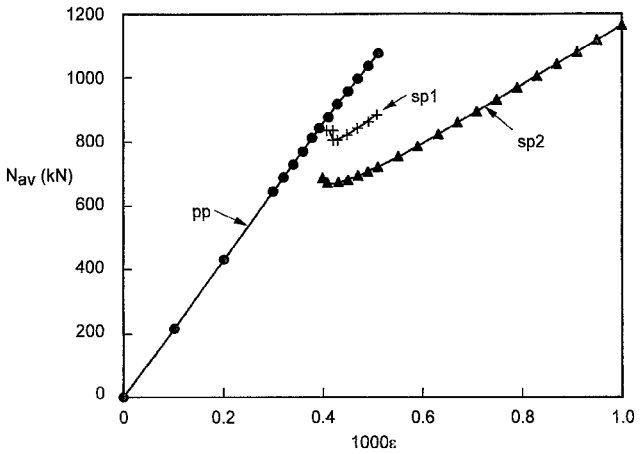

Fig. 14 Nonlinear response of the curved panel with edge stiffeners: variation of average longitudinal force with applied shortening strain.

under the action of uniform longitudinal compressive stress. On the assumption of clamped ends, and using $q = 16$, the lowest buckling load has been calculated as 971 kN. Note that other buckling modes occur in close proximity; there are eight buckling modes occurring between 971 and 997 kN. Note also that on the assumption of diaphragm ends, the calculated buckling load is 795 kN. Thus, the experimental value of buckling load lies about midway between the theoretical values based on clamped ends and on diaphragm ends.

In using the present FSM capability to predict the nonlinear response of the panel to progressive end shortening, a faceted crosswise modeling is again used with a total of 12 strips, 8 of which represent the curved portion, in the context of SDPT analysis with $q = 6$. The predicted general response of the panel (N_{av} vs ε) is shown in Fig. 14 and, as in the preceding example, reveals the stable parts of a primary path (pp) and two secondary paths (sp1 and sp2). The deformed shapes of the panel in these paths are shown in Fig. 15. Some verification of the FSM predictions is given by the deformed shape corresponding to the predicted lowest equilibrium path (sp2) (as shown in Fig. 15c) being very similar to the experimental deformed shape shown in Fig. 13b.

Conclusions

The spline FSM has been developed for the prediction of the postbuckling behavior of composite-laminated structures that are arbitrary prismatic assemblies of component flat plates that are rigidly connected together at their longitudinal edges. The development has been made on the assumption of geometrically nonlinear behavior (with nonlinear terms in v as well as w in the strain–displacement equations), and a total Lagrangian approach has been used. The properties of a finite strip may be based here on the use of classical plate theory or of first-order shear deformation plate theory, and a number of different types of finite strip models are available within each category.

The developed nonlinear capability has a quite general nature, which is aided by the increased versatility of the spline FSM as compared to the semi-analytical FSM used in earlier studies. In this paper, however, attention has been restricted to consideration of the response of structures that are subjected to a progressive uniform end shortening. Within this category of problem, the presented applications give a good idea of the scope of the developed FSM capability, which can embrace the analysis of curved panels using approximate faceted models. Available results from other sources for some of the presented applications help to confirm the validity of the FSM capability.

Acknowledgment

The authors are pleased to acknowledge the financial support of the U.K. Engineering and Physical Sciences Research Council for the work reported here.

References

[1] Dawe, D. J., "Finite Strip Buckling and Post-Buckling Analysis," *Buckling and Postbuckling of Composite Plates*, edited by G. J. Turvey and I. H. Marshall, Chapman and Hall, London, 1995, pp. 109–154.

[2] Graves-Smith, T. R., and Sridharan, S., "A Finite Strip Method for the Post-Locally-Buckled Analysis of Plate Structures," *International Journal of Mechanical Sciences*, Vol. 20, No. 2, 1978, pp. 833–842.

[3] Sridharan, S., and Graves-Smith, T. J., "Post-Buckling Analyses with Finite Strips," *Journal of Engineering Mechanics Division, ASCE*, Vol. 107, No. EM5, 1981, pp. 869–887.

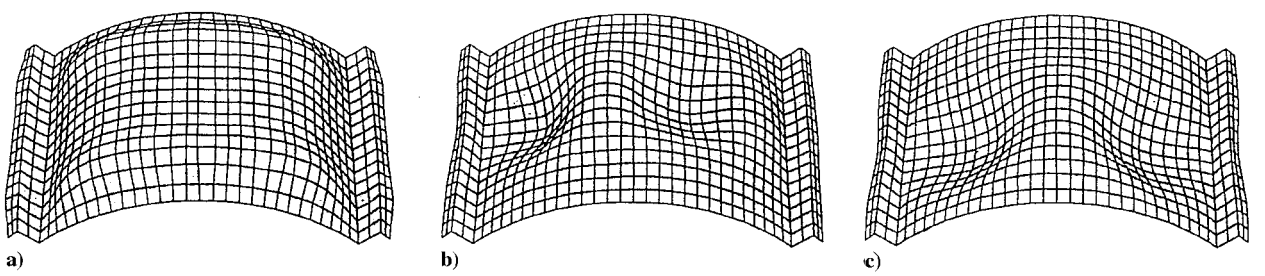

a) b) c)

Fig. 15 Deformed shapes of the curved panel with edge stiffeners: a) on pp, b) on sp1, and c) on sp2.

[4]Hancock, G. J., "Nonlinear Analysis of Thin Sections in Compression," *Journal of Structural Engineering Division, ASCE*, Vol. 107, No. ST3, 1981, pp. 455–471.

[5]Dawe, D. J., Lam, S. S. E., and Azizian, Z. G., "Non-Linear Finite Strip Analysis of Rectangular Laminates Under End Shortening, Using Classical Plate Theory," *International Journal for Numerical Methods in Engineering*, Vol. 35, No. 5, 1992, pp. 1087–1110.

[6]Lam, S. S. E., Dawe, D. J., and Azizian, Z. G., "Non-Linear Analysis of Rectangular Laminates Under End Shortening, Using Shear Deformation Plate Theory," *International Journal for Numerical Methods in Engineering*, Vol. 36, No. 6, 1993, pp. 1045–1064.

[7]Dawe, D. J., and Lam, S. S. E., "Analysis of the Post-Buckling Behaviour of Rectangular Laminates," *Proceedings of the 33rd AIAA/ASME/ASCE/AHS/ASC Structures, Structural Dynamics, and Materials Conference*, AIAA, Washington, DC, 1992, pp. 219–229.

[8]Dawe, D. J., Wang, S., and Lam, S. S. E., "Finite Strip Analysis of Imperfect Laminated Plates Under End Shortening and Normal Pressure," *International Journal for Numerical Methods in Engineering*, Vol. 38, No. 4, 1995, pp. 4193–4205.

[9]Dawe, D. J., Lam, S. S. E., and Azizian, Z. G., "Finite Strip Post-Local-Buckling Analysis of Composite Prismatic Plate Structures," *Computers and Structures*, Vol. 48, No. 6, 1993, pp. 1011–1023.

[10]Wang, S., and Dawe, D. J., "Finite Strip Large Deflection and Post-Overall-Buckling Analysis of Diaphragm-Supported Plate Structures," *Computers and Structures*, Vol. 61, No. 1, 1996, pp. 155–170.

[11]Cheung, Y. K., and Fan, S. C., "Static Analysis of Right Box Girder Bridges by Spline Finite Strip Method," *Proceedings of the Institution of Civil Engineers*, Vol. 75, Pt. 2, June 1983, pp. 311–323.

[12]Fan, S. C., and Cheung, Y. K., "Flexural Free Vibrations of Rectangular Plates with Complex Support Conditions," *Journal of Sound and Vibration*, Vol. 93, No. 1, 1984, pp. 81–94.

[13]Lau, S. C., and Hancock, G. J., "Buckling of Thin-Walled Structures by a Spline Finite Strip Method," *Thin-Walled Structures*, Vol. 4, 1986, pp. 269–294.

[14]Kwon, Y. B., and Hancock, G. J., "A Nonlinear Elastic Spline Finite Strip Analysis for Thin-Walled Sections," *Thin-Walled Structures*, Vol. 12, No. 4, 1991, pp. 295–319.

[15]Wang, S., and Dawe, D. J., "The Use of Spline Functions in Calculating the Natural Frequencies of Anisotropic Rectangular Laminates," *Composite Structures—4*, edited by I. H. Marshall, Elsevier Applied Science, London, 1987, pp. 1.447–1.460.

[16]Dawe, D. J., and Wang, S., "Buckling of Composite Plates and Plate Structures Using the Spline Finite Strip Method," *Composites Engineering*, Vol. 4, No. 11, 1994, pp. 1099–1117.

[17]Dawe, D. J., and Wang, S., "Spline Finite Strip Analysis of the Buckling and Vibration of Rectangular Composite Laminated Plates," *International Journal of Mechanical Sciences*, Vol. 37, No. 6, 1995, pp. 645–667.

[18]Wang, S., and Dawe, D. J., "Spline Finite Strip Analysis of the Buckling and Vibration of Composite Prismatic Plate Structures," *International Journal of Mechanical Sciences*, Vol. 39, No. 10, 1997, pp. 1161–1180.

[19]Dawe, D. J., and Wang, S., "Buckling and Vibration Analysis of Composite Plate and Shell Structures Using the PASSAS Software Package," *Composite Structures*, Vol. 38, Nos. 1–4, 1997, pp. 541–551.

[20]Wang, S., and Dawe, D. J., "Buckling of Composite Shell Structures Using the Spline Finite Strip Method," *Composites: Part B*, Vol. 30, 1999, pp. 351–364.

[21]Dawe, D. J., and Wang, S., "Postbuckling Analysis of Thin Rectangular Laminated Plates by Spline FSM," *Thin-Walled Structures*, Vol. 30, Nos. 1–4, 1998, pp. 159–179.

[22]Wang, S., and Dawe, D. J., "Spline FSM Post-Buckling Analysis of Shear-Deformable Rectangular Laminates," *Thin-Walled Structures*, Vol. 34, No. 2, 1999, pp. 163–178.

[23]Novozhilov, V. V., *Foundations of Nonlinear Theory of Elasticity*, Greylock, Rochester, NY, 1953.

[24]Whitney, J. M., and Pagano, N. J., "Shear Deformation in Heterogeneous Anisotropic Plates," *Journal of Applied Mechanics*, Vol. 37, Dec. 1970, pp. 1031–1036.

[25]Whitney, J. M., "Shear Correction Factors for Orthotropic Laminates under Static Load," *Journal of Applied Mechanics*, Vol. 40, March 1973, pp. 302–304.

[26]Dawe, D. J., and Wang, S., "Vibration of Shear-Deformable Beams Using a Spline-Function Approach," *International Journal for Numerical Methods in Engineering*, Vol. 33, No. 4, 1992, pp. 815–844.

[27]Gallagher, R. H., "Finite Element Method for Instability Analysis," *Finite Element Handbook*, edited by H. Kardestuncer and D. H. Norrie, McGraw–Hill, New York, 1987, pp. 2.249–2.273.

[28]Stroud, W. J., Greene, W. H., and Anderson, M. S., "Buckling Loads of Stiffened Panels Subjected to Combined Longitudinal Compression and Shear: Results Obtained with PASCO, EAL and STAGS Computer Programs," NASA TP2215, 1984.

[29]Peshkam, V., and Dawe, D. J., "Buckling and Vibration of Finite-Length Composite Plate Structures with Diaphragm Ends, Part II: Computer Programs and Buckling Applications," *Computer Methods in Applied Mechanics and Engineering*, Vol. 77, 1989, pp. 227–252.

[30]Snell, M. B., and Greaves, L. J. "Buckling and Strength Characteristics of Some CFRP Stiffened Curved Panels," *Thin-Walled Structures*, Vol. 11, No. 1 and 2, 1991, pp. 149–176.

A. N. Palazotto
Associate Editor